Photothermocapillary Oscillators

Adam W. Hauser, Subramanian Sundaram, and Ryan C. Hayward

Phys. Rev. Lett. **121**, 158001 — Published 12 October 2018

DOI: 10.1103/PhysRevLett.121.158001

Photothermocapillary Oscillators

Adam W. Hauser,[1,*] Subramanian Sundaram,[2,*] and Ryan C. Hayward[1,†]

[1]*Department of Polymer Science and Engineering, University of Massachusetts Amherst, Amherst, MA 01003, USA*
[2]*Department of Electrical Engineering and Computer Science, Massachusetts Institute of Technology, Cambridge, MA 02139, USA*

(Dated: September 18, 2018)

We present a new class of tunable light driven oscillators based on mm-scale objects adsorbed at fluid interfaces. A fixed light source induces photothermal surface tension gradients (Marangoni stresses) that drive nanocomposite hydrogel discs away from a stable apex position atop a drop of water. The capillary forces on the disc increase with surface curvature; thus, they act to restore the disc to its original position. As the disc re-enters the light source it again experiences Marangoni propulsion, leading to sustained oscillation for appropriate conditions. Propulsive forces can be modulated with incident light intensity, while the restoring force can be tuned via surface curvature – i.e. drop volume – providing highly tunable oscillatory behaviors. To our knowledge, this is the first example where Marangoni and capillary forces combine to incite sustained motion. As such, a model was developed that describes this behavior and provides key insights into the underlying control parameters. We expect that this simple approach will enable the study of more complex and coupled oscillatory systems.

Light-fueled machines from the molecular to the macro-scale represent an important class of devices that enable remote control using a potentially renewable fuel source without traditional chemical waste products.[1–3] On the molecular level, ring shuttling and isomerization constitute the most basic forms of photo-induced motion.[1, 2] Moving up in scale, light absorbing nano and micro particles have been shown to traverse in a liquid via photo-induced thermophoresis or 'self-thermophoresis'.[4–6] At the macroscopic level, light-triggered actuation of polymer networks has been demonstrated through a number of avenues,[7–9] but systems that exhibit sustained actuation from a static light source are thus far rare and largely limited to liquid crystal polymer networks.[10–15] While in many cases, such sustained actuation has not yielded net translation, cleverly designed boundary constraints or moving light sources have allowed for rolling,[16, 17] crawling [15, 18–21] and swimming [22–27] machines driven by light.

Photo-directed motion at an interface poses unique challenges and opportunities due to the important role played by surface tension. Photo-chemically [28] and photo-thermally [29, 30] defined surface tension gradients have been exploited to drive temporary motion at an aqueous-air interface. Less conventional approaches to light-driven interfacial motion have relied on the deformation of liquid crystal elastomer films,[31] or photothermally-induced bursting of vapor bubbles.[32] However, there are few examples to date where a static light source sustains continuous interfacial motion. Maggi and coworkers pioneered the first example of continuous rotation of asymmetric photothermally driven micro gears.[33] More recently, micro-scale oscillations of microparticles were shown to develop at high laser power where thermal gradient [34] or diffusiophoretic [35] forces begin to compete with optical trapping forces. Here, we demonstrate a new type of light-driven sustained motion in which a light-absorbing object on a curved liquid interface exhibits controlled, sustained oscillatory motion driven by a static light source. This new class of oscillators relies on propulsion by photothermal Marangoni force and a restoring capillary energy landscape that is fixed in time, but varies in space due to surface curvature. While thermocapillary effects are well known to play an important role in driving fluid recirculation in the presence of externally imposed temperature gradients[36–38], and can lead to temperature oscillations within droplets [39, 40], they have not been explored in the context of imposing oscillatory motion of adsorbed objects as presented here.

The experimental realization of photothermocapillary oscillation relies on nanocomposite gel discs situated atop water drops illuminated by white light shone vertically from below through the center of the drop. Gold nanoparticles embedded in the discs absorb and efficiently convert light to heat due to their surface plasmon resonance (SPR).[41–43] The water at the gel edge is heated and spreads on the surrounding lower temperature surface. Any deviation from azimuthal symmetry (e.g. due to non-uniformities in gel shape or nanoparticle concentration, or a small displacement of the gel) will lead to anisotropic flow about the disc at the air-water interface. When the gel is perturbed from the apex, the thermal gradient across the gel increases as the leading edge moves to lower intensities and the trailing edge closer to higher intensities – giving rise to an acceleration towards the drop perimeter. The capillary force acts as a spring and restores the gel position back to the apex. If the light remains on, the gel again begins to heat, is propelled towards the drop edge, and pushed

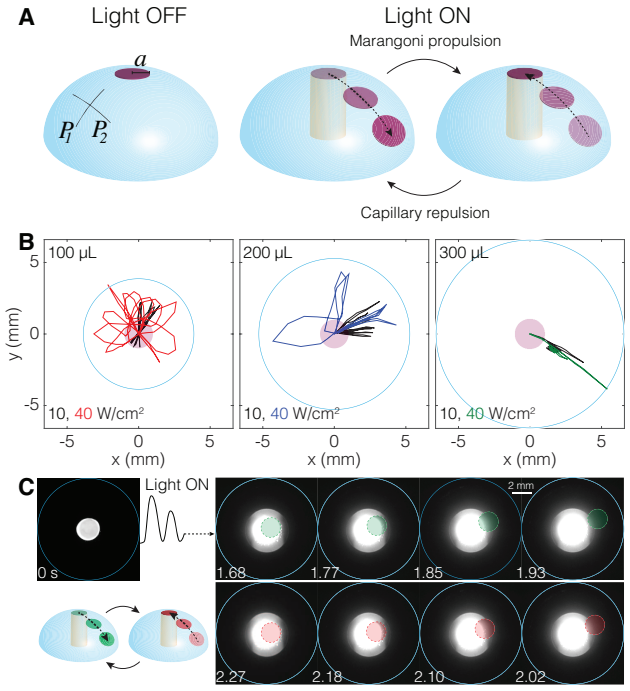

FIG. 1. A) Schematic description of photothermocapillary oscillators; B) a top view mapping of the initial 5 s of center-of-mass motion of a nanocomposite gel disc ($a = 1$ mm, size depicted in purple for reference) in projected x and y coordinates for 10 (black) and 40 W/cm^2 (colored) incident intensity; droplet volume from left to right is 100, 200 and 300 μL and perimeters are outlined in light blue; C) snap-shots of the 200 μL sample at 10 W/cm^2 intensity during its third period with the gel artificially colored to facilitate viewing and overall time since the light source was switched on noted in seconds.

back, resulting in sustained oscillatory motion for appropriate conditions (Figure 1A). Figure 1B shows the top view trajectories of a gel at 10 and 40 W/cm^2 incident intensity on different drop volumes for the initial 5 s after the light is turned on. Comparing these trajectories, it is clear that the oscillation becomes much more regular for lower light intensity and increased drop volume. Supporting movies S1 and S2 show the gel discs from the same vantage point on a 200 μL drop at 10 and 40 W/cm^2 intensity, respectively.

In the dark, the nanocomposite gels rest at the apex of the water drops. It is important to note that the drop volumes are large enough to be deformed by gravity and are thus not spherical caps. This means that the deviatoric ($\Delta c_0 = P_1 - P_2$) and mean ($H_0 = \frac{P_1+P_2}{2}$) curvatures are not constant along the surface, and in fact increase as a function of distance away from the apex. We can neglect gravitational effects on the deformation of the interface by the particle ($B_0 = \Delta\rho g a h/\gamma \sim 10^{-4}$–$10^{-5}$, h is the disc thickness and $\Delta\rho$ is the density difference between gel and water), such that the total energy of adsorbing a disc to a curved interface can be estimated as [44–46]

$$\frac{\Delta E}{\pi\gamma a^2} = \frac{a^2 H_0^2}{4} + \frac{a^2 \Delta c_0^2}{8} - h_p \Delta c_0, \qquad (1)$$

where a is the gel radius, h_p is the amplitude of the quadrupolar interface distortion from the gel [44–46]) and γ is the air-water surface tension. As the nanocomposite gel discs are planar and easily bent by surface tension, we ignore h_p and describe the capillary energy of our system as

$$\widetilde{E}_{cap} = \frac{\Delta E}{\pi\gamma a^2} \approx \frac{a^2}{8}(2H_0^2 + \Delta c_0^2), \qquad (2)$$

where $\widetilde{E}_{cap}$ is the dimensionless capillary energy that varies with the principle curvatures and thus with position (characterized by the contour length from the drop apex s), but not with time t.

To model the oscillatory dynamics, we numerically solve the coupled motion and heat transfer problem. An in-depth description can be found in the SI, but the key points are summarized here [47]. After computing the axisymmetric droplet shape for a given volume, the steady-state restoring capillary potential along the surface of the droplet is calculated from eq. 2 and the derivative with position gives the capillary force, F_{cap}. The Marangoni force, $F_{mar} \approx \gamma_T \Delta T a$ as described by Würger,[58] is computed from the temperature differential between the leading and the trailing edge of the disc. The overall force balance on the disc is

$$F_{mar}(s, \dot{s}) - F_{cap}(s) - F_{drag}(\dot{s}) = m_{eff}\ddot{s}. \qquad (3)$$

See the SI for details on the effective mass (m_{eff}) and drag (F_{drag}) terms.

Using this model, we next make a detailed comparison with experimental observations of how the oscillatory motion is tuned by key system parameters. Figure 2 shows that increased light intensity leads to a monotonic rise in frequency and amplitude when the drop volume and gel size are fixed. From the perspective of a simple harmonic oscillator, the natural frequency is defined by the spring constant and mass ($\sqrt{k_s/m}$). If we instead think of the system as a nonlinear oscillator with a stiffening spring, an increased oscillation amplitude will also increase the frequency [59] and the system is amplitude limited. This behavior is in excellent agreement with the model. Frequency scales nearly linearly over the intensity range tested, with slopes of 0.012 ± 0.005 and 0.011 ± 0.001 in experiments and model, respectively (Figure 2C). Phase portraits give additional insight into the stability of the oscillations and the quality of the model (Figure 2D). We more clearly see the velocities and attractor (closed phase space) progressively increase

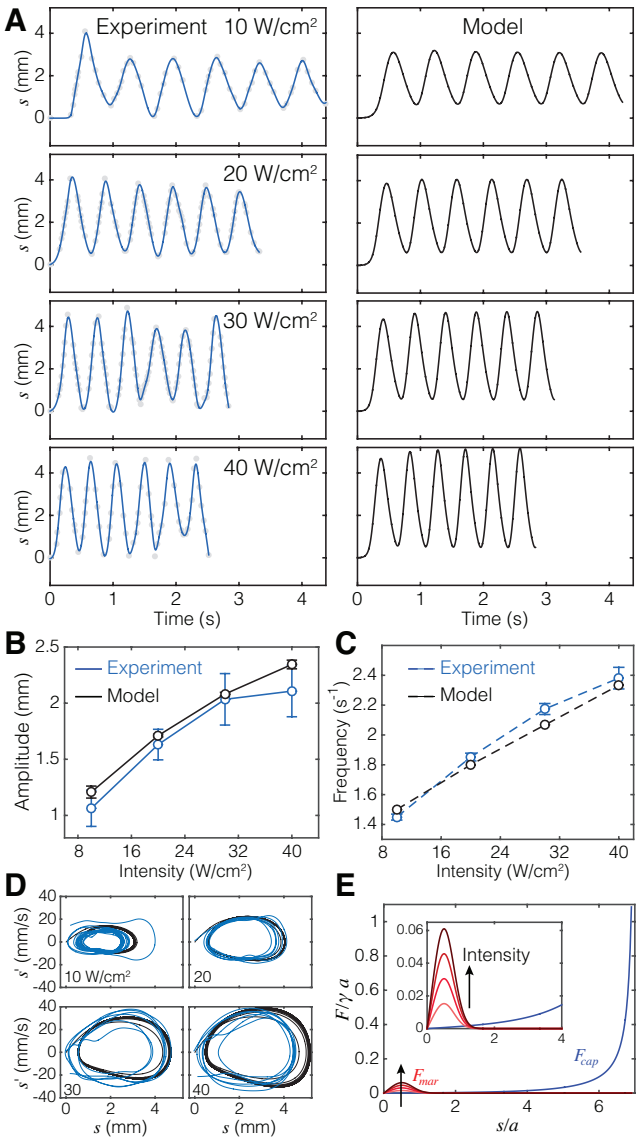

FIG. 2. A) Variation of disc center position s with time over 6 cycles on a 200 μL drop with a gel size of $a = 1$ mm at the incident intensities indicated. Dependence of amplitude (B) and frequency (C) on light intensity; D) experimental (blue) and model (black) phase portraits at each intensity; E) calculated maximum Marangoni force (F_{mar}) for the intensities shown in A-D and the capillary force (F_{cap}) landscape calculated from Eq. 2.

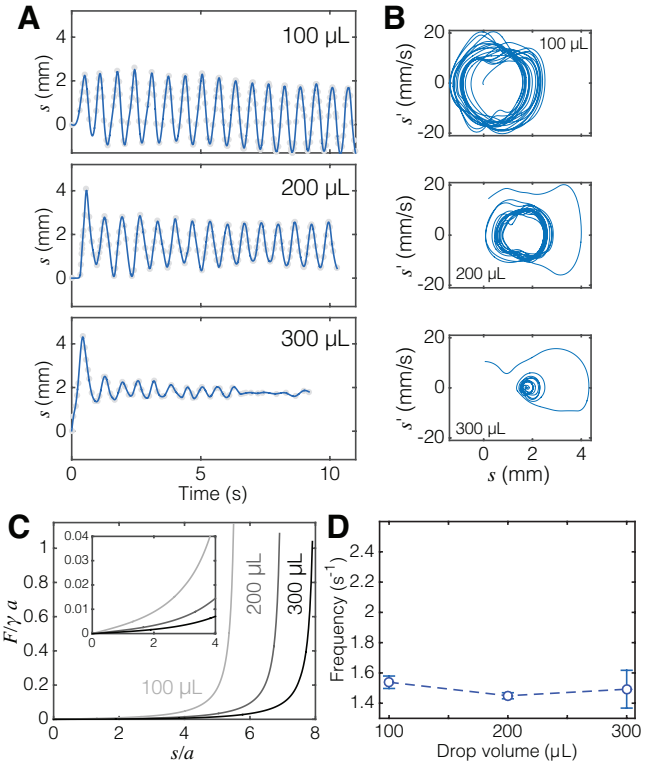

FIG. 3. A) Variation of the disc's center position s with time at 10 W/cm^2 intensity at the drop volumes indicated; B) experimental phase portraits at each volume; C) capillary force (F_{cap}) landscape at each volume calculated from Eq. 2; D) experimental dependence of oscillation frequency on drop volume.

with intensity, as does the asymmetry between positive and negative velocities (away from the apex is positive).

To further explore the system parameters, we alter the capillary force landscape by changing the drop volume from 100–300 μL. Drop heights are limited by gravity and the three phase contact lines are fixed (≈87°), so increasing volume effectively flattens the drop shape near the apex relative to the curvature near the contact line. The decreased curvature near the apex significantly weakens the restoring force at low s (see Figure 3C). With light intensity and gel size held constant, an increase in drop volume affords an increase in the apparent damping behavior, as seen in Figure 3A. In the 300 μL drop case, the importance of drag is clear, as we see the amplitude decay over time to ultimately yield a fixed steady-state position.

Conversely, we see little to no effect of drop volume on oscillation frequency. The 100 μL drop has a capillary restoring force great enough to propel the disc through the origin each period. The disc decelerates as it nears, then accelerates when it passes through, the light beam, which is evident in the phase portrait in Figure 3B. This behavior is mostly absent in the model (Figure S2), where the large restoring force does push the disc slightly through the origin, but acceleration in the opposing direction is not seen. It is worth noting that as we increase intensity in the 100 μL drop case, the oscillations become irregular and it is difficult to measure a frequency, so we are likely very near a transition to chaotic behavior (Figure 1B, Supporting Videos S3 and S4). The 300 μL case is also interesting in that it is the only case that results in a steady-state non-oscillatory position at each intensity for this disc size. With these complexities in mind, it is

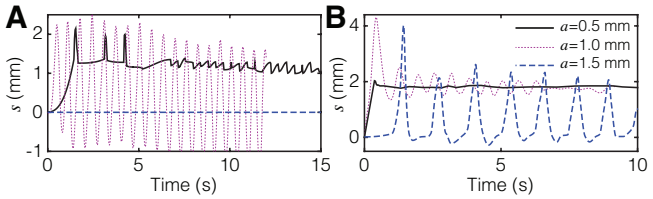

FIG. 4. A) Position s with time for 0.5, 1 and 1.5 mm gels on 100 μL and B) 300 μL drops with incident intensities adjusted to maintain equivalent heat generation.

perhaps not surprising that a simple relationship is not found between drop volume and frequency.

We next characterize the influence of gel disc size. For discs with $a = 0.5$ mm, appreciably smaller than the beam radius (1.2 mm), a steady-state position near the beam perimeter is reached without oscillating for the larger drops, but small-amplitude oscillations can be achieved on 100 μL drops (Figure 4). Due to the fall-off in light intensity away from the center of the beam, a smaller disc size translates to a lower Marangoni force due to the smaller difference in temperature between leading and trailing ends. This, in conjunction with the weaker restoring force (16 times smaller than for 1 mm discs) explains the highly damped behavior observed. Once the capillary force is large enough to restore the position far enough into a high intensity beam by reducing the drop volume to 100 μL, very small amplitude and irregular oscillations develop (Figure 4A, black curve).

On the contrary, discs larger than the light beam (a =1.5 mm) experience a larger capillary restoring force (5 times higher than for a 1 mm disc) that prevents the escape from the light beam altogether in the case of 100 and 200 μL drops, since the Marangoni force increases much more slowly with disc size ($F_{mar} \sim a$). As a result, the larger discs only experience sustained motion on 300 μL drops – the weakest capillary force landscape tested (Figure 4B). To keep the total power of light absorbed, and therefore the overall rate of heat generation constant, the intensity in these experiments was adjusted in inverse proportion to the disc area.

Although the current study has focused on understanding and modeling the oscillatory behavior of single circular discs, we anticipate that the system will provide a rich landscape for future studies on more complex behaviors. For example, we find that star-shaped gels follow a 'fishtail'-shaped oscillation pathway on 300 μL drops (Supporting Video S5). When three circular discs with $a = 1.0$ mm are placed simultaneously on a 200 μL drop, they undergo predominantly in-phase oscillations under the conditions studied, though temporary jumps to states in which one disc lags the others suggest that a variety of phase-locking behaviors may be possible under different conditions (Supporting Video S6).

We have demonstrated a new type of sustained oscillatory motion driven by a static light source. Millimeter-scale nanocomposite gel discs situated atop water drops are propelled by photothermally induced Marangoni stresses and restored by the capillary forces exerted due to interfacial curvature. Oscillation ranges from highly regular to nearly chaotic, and from sustained to damped, with light intensity, drop volume, and gel size offering convenient parameters to tune the behavior. A simplified model that couples heat generation and transfer to gel motion describes the key qualitative features of the experimental observations. We expect that this simple system can enable further studies of complex, and coupled, oscillatory behaviors.

This work was funded by the US Army Research Office through grant W911NF-16-1-0119. The authors declare no conflicts of interest.

* These authors contributed equally to this work
† hayward@umass.edu

[1] V. Balzani, A. Credi, and M. Venturi, Chem. Soc. Rev. **38**, 1542 (2009).
[2] R. Ballardini, V. Balzani, A. Credi, M. T. Gandolfi, and M. Venturi, Acc. Chem. Res. **34**, 445 (2001).
[3] H. Zeng, P. Wasylczyk, D. S. Wiersma, and A. Priimagi, Adv. Mater , 1703554 (2017).
[4] R. Golestanian, Phys. Rev. Lett. **108**, 038303 (2012).
[5] M. Xuan, Z. Wu, J. Shao, L. Dai, T. Si, and Q. He, J. Am. Chem. Soc **138**, 6492 (2016).
[6] Z. Wu, X. Lin, Y. Wu, T. Si, J. Sun, and Q. He, ACS Nano **8**, 6097 (2014).
[7] T. J. White and D. J. Broer, Nat. Mater. **14**, 1087 (2015).
[8] S.-J. Jeon, A. W. Hauser, and R. C. Hayward, Acc. Chem. Res. **50**, 161 (2017).
[9] D.-D. Han, Y.-L. Zhang, J.-N. Ma, Y.-Q. Liu, B. Han, and H.-B. Sun, Adv. Mater. **28**, 8328 (2016).
[10] S. Serak, N. Tabiryan, R. Vergara, T. J. White, R. A. Vaia, and T. J. Bunning, Soft Matter **6**, 779 (2010).
[11] K. M. Lee, M. L. Smith, H. Koerner, N. Tabiryan, R. a. Vaia, T. J. Bunning, and T. J. White, Adv. Funct. Mater. **21**, 2913 (2011).
[12] A. W. Hauser, D. Liu, K. C. Bryson, R. C. Hayward, and D. J. Broer, Macromolecules **49**, 1575 (2016).
[13] K. Kumar, C. Knie, D. Bléger, M. A. Peletier, H. Friedrich, S. Hecht, D. J. Broer, M. G. Debije, and A. P. Schenning, Nat. Commun. **7**, 11975 (2016).
[14] A. H. Gelebart, G. Vantomme, E. Meijer, and D. J. Broer, Adv. Mater. **29**, 1606712 (2017).
[15] A. H. Gelebart, D. J. Mulder, M. Varga, A. Konya, G. Vantomme, E. Meijer, R. L. Selinger, and D. J. Broer, Nature **546**, 632 (2017).
[16] M. Yamada, M. Kondo, J. I. Mamiya, Y. Yu, M. Kinoshita, C. J. Barrett, and T. Ikeda, Angew. Chem. Int. Ed. **47**, 4986 (2008).
[17] Y. Hu, G. Wu, T. Lan, J. Zhao, Y. Liu, and W. Chen, Adv. Mater. **27**, 7867 (2015).
[18] M. Yamada, M. Kondo, R. Miyasato, Y. Naka, J.-i. Mamiya, M. Kinoshita, A. Shishido, Y. Yu, C. J. Barrett, and T. Ikeda, J. Mater. Chem. **19**, 60 (2009).

[19] E. Wang, M. S. Desai, and S.-W. Lee, Nano Lett. **13**, 2826 (2013).
[20] M. Rogóż, H. Zeng, C. Xuan, D. S. Wiersma, and P. Wasylczyk, Adv. Opt. Mater. **4**, 1689 (2016).
[21] H. Zeng, O. M. Wani, P. Wasylczyk, and A. Priimagi, Macromol. Rapid Commun. **39**, 1700224 (2018).
[22] O. Kuksenok and A. C. Balazs, Adv. Funct. Mater. **23**, 4601 (2013).
[23] L. Wang, Y. Liu, Y. Cheng, X. Cui, H. Lian, Y. Liang, F. Chen, H. Wang, W. Guo, and H. Li, Adv. Sci. **2**, 1500084 (2015).
[24] C. Huang, J.-a. Lv, X. Tian, Y. Wang, Y. Yu, and J. Liu, Sci. Rep. **5**, 17414 (2015).
[25] A. W. Hauser, A. A. Evans, J.-H. Na, and R. C. Hayward, Angew. Chem. Int. Ed. **54**, 5434 (2015).
[26] S.-J. Park, M. Gazzola, K. S. Park, S. Park, V. Di Santo, E. L. Blevins, J. U. Lind, P. H. Campbell, S. Dauth, and A. K. Capulli, Science **353**, 158 (2016).
[27] S. Palagi, A. G. Mark, S. Y. Reigh, K. Melde, T. Qiu, H. Zeng, C. Parmeggiani, D. Martella, A. Sanchez-Castillo, and N. Kapernaum, Nat. Mater. **15**, 647 (2016).
[28] A. Diguet, R.-M. Guillermic, N. Magome, A. Saint-Jalmes, Y. Chen, K. Yoshikawa, and D. Baigl, Angew. Chem. Int. Ed. **48**, 9281 (2009).
[29] D. Okawa, S. J. Pastine, A. Zettl, and J. M. J. Fréchet, J. Am. Chem. Soc. **131**, 5396 (2009).
[30] M. Ichikawa, F. Takabatake, K. Miura, T. Iwaki, N. Magome, and K. Yoshikawa, Phys. Rev. E **88**, 012403 (2013).
[31] M. Camacho-Lopez, H. Finkelmann, P. Palffy-Muhoray, and M. Shelley, Nat. Mater. **3**, 307 (2004).
[32] F. Meng, W. Hao, S. Yu, R. Feng, Y. Liu, F. Yu, P. Tao, W. Shang, J. Wu, C. Song, and T. Deng, J. Am. Chem. Soc. **139**, 12362 (2017).
[33] C. Maggi, F. Saglimbeni, M. Dipalo, F. De Angelis, and R. Di Leonardo, Nat. Commun. **6**, 7855 (2015).
[34] M.-C. Zhong, Z.-Q. Wang, and Y.-M. Li, Opt. Express **25**, 2481 (2017).
[35] F. Schmidt, A. Magazz, A. Callegari, L. Biancofiore, F. Cichos, and G. Volpe, Phys. Rev. Lett. **120**, 068004 (2018).
[36] L. Pismen, Phys. Rev. Lett. **59**, 2740 (1987).
[37] A. A. Nepomnyashchy and I. B. Simanovskii, J. Fluid. Mech. **805**, 322 (2016).
[38] M. Lappa, Int. J. Therm. Sci. **118**, 303 (2017).
[39] Y. Kita, A. Askounis, M. Kohno, Y. Takata, J. Kim, and K. Sefiane, Appl. Phys. Lett. **109**, 171602 (2016).
[40] J. Wang, L. Duan, and Q. Kang, Chin. Phys. Lett. **34**, 074703 (2017).
[41] A. O. Govorov, W. Zhang, T. Skeini, H. Richardson, J. Lee, and N. A. Kotov, Nanoscale Res. Lett. **1**, 84 (2006).
[42] S. Eustis and M. A. El-Sayed, Chem. Soc. Rev. **35**, 209 (2006).
[43] Y. Zhou, A. W. Hauser, N. P. Bende, M. G. Kuzyk, and R. C. Hayward, Adv. Funct. Mater. **26**, 5447 (2016).
[44] M. Cavallaro, L. Botto, E. P. Lewandowski, M. Wang, and K. J. Stebe, Proc. Natl. Acad. Sci. **108**, 20923 (2011).
[45] P. Galatola, Soft Matter **12**, 328 (2016), arXiv:arXiv:1502.01672.
[46] A. Würger, Phys. Rev. E **74**, 041402 (2006).
[47] See Supplemental Material [url] for a complete description of the model, and additional information on different forces and simulation settings - which includes Refs. [48-57].
[48] N. Zheng, J. Fan, and G. D. Stucky, J. Am. Chem. Soc. **128**, 6550 (2006).
[49] O. Del Rıo and A. Neumann, J. Colloid Interface Sci. **196**, 136 (1997).
[50] Y. Cøengel, *Heat transfer: a practical approach* (McGraw-Hill, New York, 2002).
[51] H. Lamb, *Hydrodynamics* (Cambridge University Press, Cambridge, 1916).
[52] K. D. Danov, R. Dimova, and B. Pouligny, Phys. Fluids **12**, 2711 (2000).
[53] A. Hajimiri and T. H. Lee, *The design of low noise oscillators* (Springer Science & Business Media, 1999).
[54] C. Chen, S. Lee, V. V. Deshpande, G.-H. Lee, M. Lekas, K. Shepard, and J. Hone, Nature nanotechnology **8**, 923 (2013).
[55] P. Steeneken, K. Le Phan, M. Goossens, G. Koops, G. Brom, C. Van der Avoort, and J. Van Beek, Nature Physics **7**, 354 (2011).
[56] X. Feng, C. White, A. Hajimiri, and M. L. Roukes, Nature nanotechnology **3**, 342 (2008).
[57] S. Sundaram and D. Weinstein, IEEE transactions on ultrasonics, ferroelectrics, and frequency control **62**, 1554 (2015).
[58] A. Würger, J. Fluid Mech. **752**, 589 (2014).
[59] R. H. Rand (Cornell University, Dept. Theoretical & Applied Mechanics, 2012).